Ab Initio Characterization of (CH₃IO₃) Isomers and the CH₃O₂ + IO Reaction Pathways

Evangelos Drougas and Agnie M. Kosmas*

Division of Physical Chemistry, Department of Chemistry, University of Ioannina, Greece 45110

Received: December 5, 2006; In Final Form: February 28, 2007

The geometries, harmonic vibrational frequencies, relative energetics, and enthalpies of formation of (CH₃IO₃) isomers and the reaction CH_3O_2 + IO have been investigated using quantum mechanical methods. Optimization has been performed at the MP2 level of theory, using all electron and effective core potential, ECP, computational techniques. The relative energetics has been studied by single-point calculations at the CCSD(T) level. Methyl iodate, CH_3OIO_2, is found to be the lowest-energy isomer showing particular stabilization. The two nascent association minima, CH_3OOOI and CH_3OOIO, show similar stabilities, and they are considerably higher located than CH_3OIO_2. Interisomerization barriers have been determined, along with the transition states involved in various pathways of the reaction CH_3O_2 + IO.

1. Introduction

The systematic observations of I_2, CH_2I_2, IO, and OIO formation in the marine boundary layer[1−2] and the potential role of iodine compounds in tropospheric ozone depletion cycles,[3−6] have stimulated an increasing interest in the reactivity of iodine containing species. The reactions of IO, in particular with itself, HO_2 and NO_2, have been examined in detail and have been shown to be important processes affecting the concentrations of ozone in the lower atmosphere.[3−4] Lately, significant contribution to tropospheric ozone removal has also been suggested to result from the reactions of IO with various organic peroxy radicals.[7] Several experimental studies reported recently have investigated the coupling of IO with the methylperoxy, CH_3O_2, perfluoromethylperoxy, CF_3O_2, and ethylperoxy radicals and measured the corresponding rate coefficients.[8−10]

Two of the experimental studies have shown that the reactions RO_2 + IO are fast and may indeed have an important impact in ozone chemistry. Bale et al.[8] measured the rate constant of the system CH_3O_2 + IO at room temperature under 2.5 Torr He diluent and obtained the value $k = (6.0 \pm 1.3) \times 10^{-11}$ cm³ molecule⁻¹ s⁻¹. Enami et al.[9] found the value $k = (7.0 \pm 3.0) \times 10^{-11}$ cm³ molecule⁻¹ s⁻¹ at 298 K and 100 Torr of N_2 diluent, in good agreement with the previous one. No significant pressure dependence was observed at 30−130 Torr of N_2, but a weak positive temperature dependence was obtained in the range 213−298 K.[9] Very recently, Dillon et al.[10] obtained a much lower rate constant, $k = (2 \pm 1) \times 10^{-12}$ cm³ molecule⁻¹ s⁻¹ at 298 K and in the pressure range 30−318 Torr N_2, i.e., about 30 times smaller than the former measurements. The difference is quite large and indicates the complexity of the system. All studies were unable to determine specific reaction pathways and analyze products and branching ratios. The investigation by Enami et al.[9] has produced only an upper limit branching ratio, <0.1, for the OIO radical formation. The lack of information on the products and the serious discrepancy over the rate constant measurements, which is directly connected to the atmospheric significance of these reactions, make desirable the theoretical study of the RO_2 + IO system and the computational investigation of its reaction pathways.

In the present work, a quantum mechanical characterization of the isomers of (CH₃IO₃) family and the related reaction between the most abundant organic peroxy radical, the methylperoxy radical, CH_3O_2 and IO, is carried out. The system is analogous to the reactions of CH_3O_2 with the ClO, BrO radicals for which several experimental and theoretical studies were reported.[11−19] It also bears similarities with the well studied HO_2 + IO reaction,[20−25] which has been found to display a large rate coefficient,[22] $k = 7.1 \times 10^{-11}$ cm³ molecule⁻¹ s⁻¹ at 298 K and has been suggested to proceed through the formation of the bound complexes, HOOOI and HOOIO.[23,25] In analogy to these studies, structures of possible intermediates are investigated, and their chemical pathways are examined using ab initio computational methods, as described in the following sections.

2. Computational Details

The MP2 level of theory[26] has been employed to carry out the optimizations of the isomeric forms and all species involved in the CH_3O_2 + IO reaction while the energetics has been investigated using single-point CCSD(T) calculations. All computations have been performed using the Gaussian 98 series of programs.[27]

Two series of optimizations have been made in this study. The first one has been an all-electron treatment employing the Sadlej-PVTZ basis sets for all atoms involved including I.[28] In the second series of optimizations, the LANL2DZ basis set has been used for I, which is based on the Hay-Wadt relativistic effective core potential[29] and which has been augmented for the purpose of the present computations with a set of uncontracted s and p diffuse functions (exponents 0.0569 and 0.0330 respectively) and d and f polarization functions (exponents 0.292 and 0.441, respectively).[30] The resulting basis set is denoted hereafter as LANL2DZspdf. The remaining atoms, C, O and H, have been treated with the standard 6-311++G(d,p) basis set.

Harmonic vibrational frequencies for all species have been determined at the MP2/Sadlej-PVTZ. Transition state configurations have been identified by one imaginary frequency as first-order saddle points and IRC calculations[31] have confirmed that the transition states determined connect the desired reactants and products. Selected transition states have also been verified at the higher MP2/LANL2DZspdf basis set level as we shall see in the next section. The relative energetics has been studied
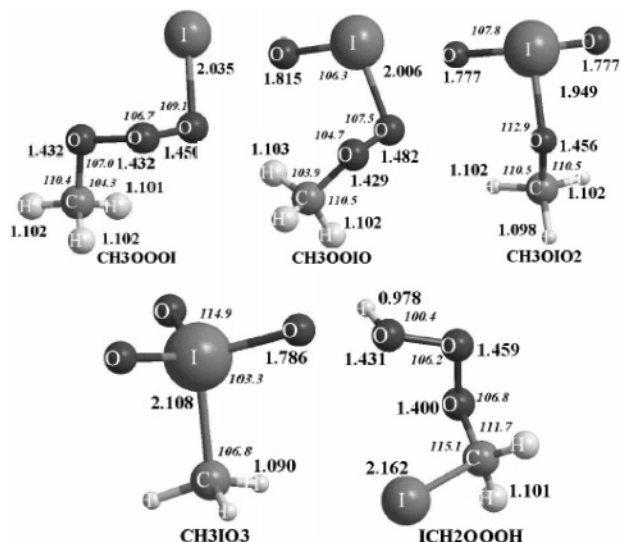
(CH$_3$IO$_3$) Isomers and the CH$_3$O$_2$ + IO Reaction Pathways

J. Phys. Chem. A, Vol. 111, No. 17, 2007 **3403**

Figure 1. Structures of isomers of the (CH$_3$IO$_3$) family at the MP2/Sadlej-PVTZ level
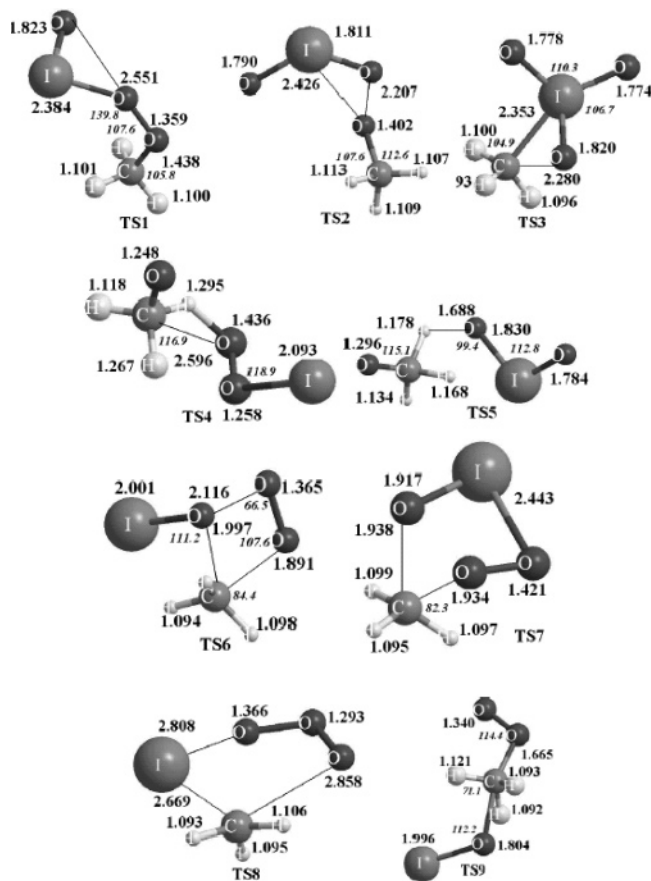

Figure 2. Structures of the transition state configurations in the reaction CH$_3$O$_2$ + IO at the MP2/Sadlej-PVTZ level

using single-point CCSD(T)/Sadlej-PVTZ//MP2/Sadlej-PVTZ and CCSD(T)/LANL2DZspdf//MP2/LANL2DZspdf calculations. The spin−orbit coupling correction for IO[32,36−37] (half the $^2\Pi_{1/2}-^2\Pi_{3/2}$ energy splitting) was taken explicitly into account in the resulting energy differences.

3. Results and Discussion

The geometries of the energy minima and the transition states are depicted in Figures 1 and 2, respectively, while the reaction energy profile is depicted in Figure 3.
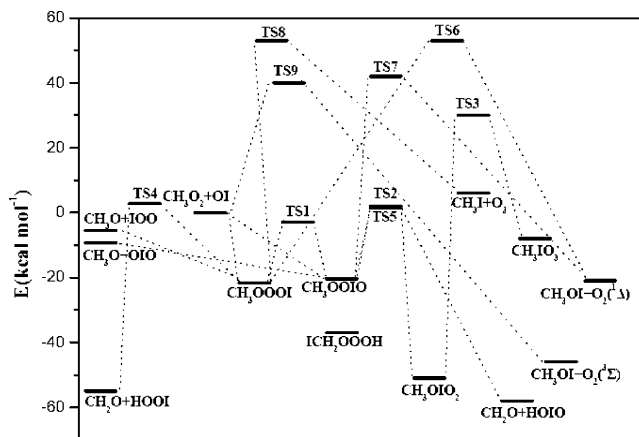

Figure 3. Energy profile of the reaction CH$_3$O$_2$ + IO at the CCSD-(T)/LANL2DZspdf level

Selected structural parameters and harmonic vibrational frequencies are summarized in Tables 1 and 2. A good overall agreement in the optimized parameters is observed between the two methodologies with a finer description by the higher MP2/LANL2DZspdf basis set level. Table 3 presents the calculated energy differences and the relative energies incorporating the spin−orbit correction for IO, which corresponds roughly to 2.2 kcal mol^{-1} and modifies all relative stabilities by this amount.

The study of the singlet surface requires the calculation of the oxygen molecule in the $^1\Delta_g$ state. The computations employing the standard basis sets fail to predict the correct experimental spacing, 22.5 kcal mol^{-1}, between singlet and triplet oxygen. They usually, produce a higher value around 30 kcal mol^{-1}.[33] This calculation can been achieved with the use of complex orbitals at the RMP2/LANL2DZ level of theory which produces a theoretical spacing value of 22.4 kcal mol^{-1}, in excellent agreement with the experimental result.

Energy Minima and Isomerization Transition States. Four isomeric energy minima have been located on the potential energy surface of the reaction CH$_3$O$_2$ + IO. They correspond to the following molecular structures: CH$_3$OOOI, CH$_3$OOIO, and CH$_3$OIO$_2$, CH$_3$IO$_3$. For completion reasons a fifth isomer, ICH$_2$OOOH, has been also examined.

The two nascent association minima are CH$_3$OOOI and CH$_3$-OOIO. The equilibrium ground state configuration of CH$_3$OOOI presents a skew geometry with COOO and OOOI dihedral angles equal to 75.2° (78.0°) and 73.4° (72.5°) at the MP2/Sadlej-PVTZ (MP2/LANL2DZspdf) level, respectively. In the following the results in parentheses are calculated by using the MP2/LANL2DZspdf methodology. The O−I bond distance is rather large, 2.035 (2.008) Å, compared to the calculated 1.891 Å and experimental 1.868 Å value in free IO.[32] The two peroxide bond lengths, CO−O and O−OI, are calculated to be 1.432 (1.415) and 1.449 (1.428) Å, respectively. The complex is located at −21.7 (−14.7) kcal mol^{-1} at the CCSD(T)/Sadlej-PVTZ (CCSD(T)/LANL2DZspdf) level below the reactants CH$_3$O$_2$ + IO. This energy difference is reduced to −19.5 (−12.5) kcal mol^{-1} when the spin−orbit correction for IO is taken into account. The second association minimum, CH$_3$-OOIO, also possesses a skew geometry with COOI and OOIO dihedral angles equal to 102.4° (98.4°) and −79.6° (−85.3°), respectively. It contains hypervalent iodine, i.e., an iodine atom presenting more than eight electrons in the valence shell. It displays quite different equilibrium distances for the two bonds between iodine and oxygen atoms. These bonds may be described as involving a bridged and a terminal oxygen atom and are found to be OO−IO = 2.006 (1.976) Å and OI−O =

TABLE 1: Selected Important Structural Parameters for (CH₃IO₃) Isomers (Å, deg), at the MP2/Sadlej-PVTZ (First Line) and MP2/LANL2DZspdf (Second Line) Levels of Theory

	C−I	C−O	O−O	O−I	I−O	−COO	−OOI	−COI	−OIO	−CIO	φ^a
CH₃OOOI		1.432	1.450	2.035		107.0	109.1				75.2
		1.426	1.428	2.008		107.6	110.5				78.0
CH₃OOIO		1.429	1.482	2.006	1.815	104.7	107.5		106.3		102.4
		1.422	1.460	1.976	1.776	106.1	109.5		107.7		98.4
CH₃OIO₂		1.456		1.949	1.777			112.9	107.8		56.3
		1.447		1.908	1.736			114.8	101.9		56.0
CH₃IO₃	2.108			1.786					114.9	103.3	
	2.072			1.729					114.3	104.0	
ICH₂OOOH	2.162	1.401	1.459			106.8					81.2
	2.129	1.389	1.441			105.4					84.5
TS1		1.438	2.551	2.384	1.823	107.6	139.8		64.1		70.1
		1.431	2.523	2.395	1.817	104.9	136.7		59.9		71.2
TS2		1.402	2.207	1.811	1.790	137.9	75.3		115.1		150.0
		1.398	2.201	1.790	1.783	135.6	73.9		114.6		145.8
TS3	2.353	2.280		1.820	1.778			67.8	106.7	82.0	150.5
	2.358	2.266		1.814	1.765			62.5	104.8	80.3	158.3
TS4		1.248	1.258	2.093			118.9				175.1
		1.255	1.276	2.088			116.4				170.8
TS5		1.296		1.830	1.784				112.8		172.4
		1.295		1.824	1.786				113.7		174.2
TS6		1.891	1.365	2.001		107.6	102.4	110.1			99.2
		1.888	1.330	2.005		108.9	100.5	110.9			100.5
TS7		1.934	1.421	2.443	1.917	109.4	83.6	107.5	72.4		70.2
		1.952	1.420	2.431	1.906	109.5	84.1	107.8	74.3		72.3
TS8	2.669	2.858	1.293	2.808		107.8	100.3				155.6
	2.654	2.861	1.287	2.775		106.4	100.8				154.2
TS9		1.665	1.340	1.996		112.5		111.4			90.5
		1.654	1.318	1.992		113.7		112.8			91.2

^{a} φ represents the C atom containing dihedral angle

TABLE 2: MP2/Sadlej-PVTZ Harmonic Vibrational Frequencies (cm⁻¹) for the (CH₃IO₃) Isomers and Important Stationary Points on the Potential Energy Surface of the Reaction CH₃O₂ + IO

CH₃OOOI	66, 136, 216, 244, 445, 542, 575, 705, 861, 1037, 1199, 1227, 1474, 1487, 1534, 3084, 3184, 3204
CH₃OOIO	67, 92, 189, 209, 273, 459, 496, 800, 915, 1047, 1201, 1228, 1472, 1490, 1537, 3068, 3164, 3190
CH₃OIO₂	30, 81, 188, 256, 287, 356, 499, 949, 956, 1020, 1183, 1190, 1482, 1499, 1530, 3069, 3158, 3201
CH₃IO₃	94, 187, 187, 278, 278, 296, 551, 897, 897, 910, 957, 957, 1310, 1457, 1457, 3103, 3236, 3236
ICH₂OOOH	77, 96, 253, 380, 470, 515, 590, 769, 874, 929, 1075, 1287, 1314, 1421, 1459, 3142, 3234, 3804
TS1^a	131i, 49, 89, 126, 197, 402, 511, 965, 982, 1095, 1175, 1218, 1474, 1483, 1511, 3060, 3160, 3209
	124i, 110, 158, 176, 174, 460, 527, 899, 941, 1014, 1192, 1227, 1384, 1493, 1517, 2983, 3079, 3125
TS2^a	149i, 64, 144, 186, 216, 269, 434, 831, 986, 1079, 1117, 1187, 1435, 1491, 1518, 2984, 3046, 3083
	155i, 103, 150, 201, 254, 303, 430, 743, 909, 1071, 1121, 1186, 1437, 1495, 1520, 2986, 3050, 3085
TS3	684i, 68, 127, 238, 272, 308, 409, 742, 824, 934, 950, 995, 1222, 1438, 1486, 3121, 3268, 3320
TS4	1265i, 57, 120, 190, 232, 376, 491, 648, 970, 1136, 1303, 1334, 1494, 1534, 1605, 1674, 1995, 2955
TS5	516i, 104, 138, 187, 247, 361, 507, 610, 867, 968, 1212, 1251, 1309, 1476, 1496, 2441, 2772, 2831
TS6	956i, 109, 177, 240,, 256, 264, 515, 571, 687, 801, 1026, 1103, 1350, 1474, 1535, 3089, 3196, 3275
TS7	948i, 168, 187, 275, 290, 435, 523, 630, 725, 929, 1019, 1068, 1335, 1467, 1533, 3097, 3216, 3277
TS8	847i, 32, 185, 227, 249, 323, 366, 709, 787, 916, 1231, 1262, 1440, 1491, 2116,
TS9	1450i, 69, 110, 277, 315, 355, 411, 556, 608, 1006, 1223, 1281, 1315, 1405, 1584, 2964, 3239, 3316

^{a} Calculated frequencies at the MP2/LANL2DZspdf level are also included for the important transition state configurations TS1 and TS2.

1.815 (1.776) Å, respectively. The different bond lengths correspond to the two different types of I−O bonding and reflect the large degree of double bond character in OI−O that involves the terminal oxygen atom. CH₃OOIO is closely located in energy to CH₃OOOI, taking into account the uncertainty of the computations, exactly like the isomers HOOOI and HOOIO.[25] This important feature implies that the reaction CH₃O₂ + IO may proceed through either association minimum with equal probability, presenting this way a different behavior from the analogous Cl and Br systems. In the latter, the hypervalent structures CH₃OOXO (X=Br, Cl) have been calculated to lie ~12 kcal mol⁻¹ higher than the normal valent adducts CH₃-OOOX at the G2 and G2MP2 levels of theory.[17,19] Hence, the mechanism of the reactions CH₃O₂ + XO (X=Br, Cl) has been suggested to involve mainly the normal valent peroxide complexes, while the reaction CH₃O₂ + IO may proceed through either association minimum with equal probability. Isomerization between CH₃OOOI and CH₃OOIO may take place through

transition state TS1 resulting from the elongation of the peroxide O−OI bond to 2.551 (2.523) Å and the approach of I to the middle oxygen atom in CH₃OOOI at 2.384 (2.395) Å. TS1 is located below reactants at −3.2 (−2.8) kcal mol⁻¹ (−1.0 (−0.6) kcal mol⁻¹, including the spin−orbit correction for IO), making the interisomerization feasible in principle, during the reaction. The calculated free energy change, ΔG, at the CCSD(T)/LANL2DZspdf level for the isomerization process CH₃OOOI → CH₃OOIO is found to be −1.2 kcal mol⁻¹ at 298 K and 0.5 kcal mol⁻¹ at 220 K. These values indicate a nearly thermoneutral process consistent with a similar and feasible participation of both isomers in the mechanism of the reaction.

The most stable isomer is methyl iodate, CH₃OIO₂, which also contains hypervalent iodine−oxygen bonds and shows particular stabilization, lying at −51.6 (−50.8) kcal mol⁻¹ below reactants and about −30 kcal mol⁻¹ below the isomers CH₃-OOOI and CH₃OOIO. The hypervalent character is again reflected in the structural characteristics which are different for

TABLE 3: Relative Energetics[a] (kcal mol^{-1}) of (CH_3IO_3) Isomers and Reactants, and Products and Transition State Barriers for the CH_3O_2 + IO Reaction Pathways, Including ZPE Corrections (kcal mol^{-1})

	MP2/ Sadlej-PVTZ	CCSD(T)/ Sadlej-PVTZ	CCSD(T)/ LANL2DZspdf	reported values[b]	ZPE
CH_3O_2 + IO[c]	0.0	0.0	0.0		28.8
CH_3OOOI	−42.1	−21.7 (−19.5)	−14.7 (−12.5)		30.3
CH_3OOIO	−44.1	−20.4 (−18.2)	−14.3 (−12.1)		29.9
CH_3OIO_2	−81.0	−51.6 (−49.4)	−50.8 (−48.6)		29.8
CH_3IO_3	−35.4	−8.4 (−6.2)	−9.5 (−7.3)		29.0
ICH_2OOOH	−62.5	−37.9 (−35.7)	−38.1 (−35.9)		31.0
TS1	−27.2	−3.2 (−1.0)	−2.8 (−0.6)		29.6
TS2	−24.1	1.9 (4.1)	2.1 (4.3)		28.7
TS3	8.2	29.9 (32.1)	33.4 (35.6)		28.2
TS4	−20.3	2.8 (5.0)	3.4 (5.6)		25.9
TS5	−26.3	1.5 (3.7)	1.9 (4.1)		28.1
TS6	25.2	53.6 (55.8)	60.2 (62.4)		26.9
TS7	11.1	42.1 (44.3)	55.3 (57.5)		28.9
TS8	15.3	53.7 (55.9)	56.4 (58.6)		30.1
TS9	15.4	40.2 (42.4)	48.0 (50.2)		28.7
CH_3O + IOO	−23.4	−6.5 (−4.3)	−5.5 (−3.2)	−2.7	27.5
CH_3O + OIO	−36.0	−10.4 (−8.2)	−9.9 (−7.7)	−7.3	27.1
CH_3I + O_3	−25.7	6.2 (8.4)	6.1 (8.3)	7.6	29.3
CH_3OI + $O_2(^1D)$	−45.1	−24.2 (−22.0)	−20.5 (−18.3)		28.0
CH_3OI + $O_2(^3)$	−67.5	−46.6 (−44.4)	−42.9 (−40.7)	−41.1	28.3
CH_2O + HOOI	−72.7	−55.5 (−53.3)	−53.4 (−51.2)	−59.6	27.0
CH_2O + HOIO	−77.9	−58.7 (−56.5)	−57.1 (−54.9)		26.0

[a] The numbers in parentheses give the relative energies that include the split-orbit energy correction factor for IO.[32,35−37]　[b] The reported heats of reaction, ΔH_r^{298}, are taken from ref 8.　[c] The reactants electronic energies are −7183.07948, −7183.04606, and −276.13953 Hartrees.

the two types of I−O bonds with bridged and terminal oxygen atoms, respectively, as in the CH_3OOIO case. Thus, very different bond distances are obtained, 1.949 (1.908) Å for CO−I compared to 1.777 (1.736) Å for OI−O. On the basis of the calculated reaction energy for dissociation to CH_3O_2 + IO at 298 K, the split-orbit energy correction for IO and the literature values for the enthalpies of formation of CH_3O_2 and IO, we can estimate the heat of formation for methyl iodate, which is a very important quantity related to the atmospheric impact of the compound. The reliable determination of ΔH_f (CH_3OIO_2) is handicapped however, by the lack of accurate information on ΔH_f (CH_3O_2) and ΔH_f (IO). Guha and Francisco[17] have adopted the estimate ΔH_f (CH_3O_2) = 24.0 kcal mol^{-1} while Knyazev and Slagle[34] have calculated ΔH_f (CH_3O_2) = 2.1 ± 1.2 kcal mol^{-1}. The two values are substantially different. Also, the literature reported values for ΔH_f (IO) differ considerably from 25.6 to 41.8 kcal mol^{-1}.[35−37] Using the most frequently quoted value for IO, ΔH_f (IO) = 27.7 ± 1.2 kcal mol^{-1},[35] we have calculated the heat of formation for methyl iodate at 298 K to be equal to 4.2 ± 2.4 kcal mol^{-1}, adopting Guha and Francisco' s ΔH_f (CH_3O_2). Accepting the value calculated by Knyazev and Slagle for the heat of formation of CH_3O_2, ΔH_f (CH_3OIO_2) is found equal to −17.7 (−16.9) ± 2.4 kcal mol^{-1} at 298 K. Comparison with the $HOIO_2$ species,[23,25] which was found to present a ΔH_f^{298} equal to −20.1 kcal mol^{-1}[25] makes us to incline to the second evaluation, ΔH_f (CH_3OIO_2) = −17.7 (−16.9) ±2.4 kcal mol^{-1}. Indeed, like the iodic acid, $HOIO_2$, which is a white powdered solid at room temperature,[38] methyl iodate exhibits the particular stabilization achieved by several -XO_2 structures (X=Cl, Br). The halogen atom in these species is considered to present the optimum hypervalent state. As discussed by Lee et.,[39] the X−O bonding, with O being a terminal oxygen atom, results from a partial p→d promotion of the lone-pair electrons in the halogen and is highly ionic. This promotion is suggested to involve the lowest energetic cost for the −XO_2 structures where a second pair electrons is promoted relative to −XO isomers. In the former systems, when the hypervalent halogen combines with a highly electronegative partner, like another halogen atom or the HO and CH_3O

moieties,[40−41] the strong ionic character of the X−O bond produces the highest stabilization. The effect is particularly enhanced in the case of the iodine compounds $HOIO_2$ and CH_3OIO_2. The examination of the Mulliken atomic charge distributions in these species shows a large positive charge on the hypervalent iodine bound to the electronegative HO and CH_3O fragments, much larger than on either Cl or Br in the corresponding hypervalent chlorinated and brominated species. Consequently, CH_3OIO_2 must show a similar stability as $HOIO_2$ and may also be considered as a possible sink compound for iodine in the troposphere.

Methyl iodate may be formed from CH_3OOIO through the isomerization transition state TS2 resulting from the breaking of the peroxy bond, 2.207 (2.201) Å and the approach of I to the oxygen connected with the carbon atom at 2.426 (2.412) Å. The corresponding barrier is relatively low located at 4.1 (4.3) kcal mol^{-1} above products including the IO spin−orbit energy correction factor. This means a feasible isomerization during the reaction and a possible reaction pathway leading to methyl iodate production under suitable temperature and pressure conditions.

The two last isomers examined are CH_3IO_3 and ICH_2OOOH. In the former, iodine promotes the third and last available valence lone pair electrons, a procedure which is not energetically as favored[39] as the promotion of the second pair electrons. As a result, CH_3IO_3 is the most unstable isomer in the family, containing only hypervalent I−O bonds. It still lies below reactants, at −8.4 (−9.5) kcal mol^{-1}, opposite to CH_3BrO_3 and CH_3ClO_3 structures which are located considerably higher than CH_3O_2 + BrO[17] and CH_3O_2 + ClO.[19] CH_3IO_3 may be formed from the isomerization of CH_3OIO_2 via transition state TS3, resulting from the elongation of the C−O bond from 1.456 (1.447) Å in CH_3OIO_2 to 2.280 (2.266) Å in TS3 and the migration of I to C atom at 2.353 (2.358) Å. The associated barrier is much higher than the reactants impying a negligible probability for this process.
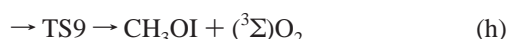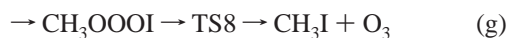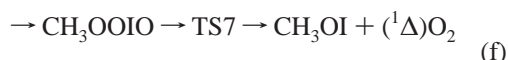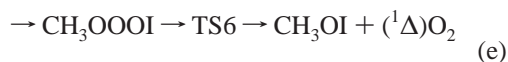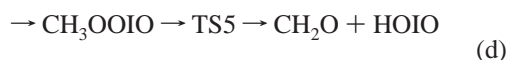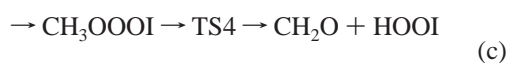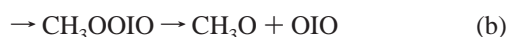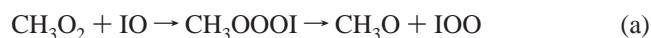
For completion purposes a final isomer in the (CH_3IO_3) family has been studied, the hydroperoxide derivative of the iodomethoxy radical, ICH_2OOOH, located at −37.9 (−38.1) kcal

mol^{-1} below reactants. The structure shows the shortest C−O distance, 1.401 (1.389) Å, among all isomers and a considerable stability, being the next stable isomer in the family after methyl iodate. Its high stability may be attributed to the electron withdrawing effect of the halogen attached to the carbon atom and the subsequent increase of the −O−H bond energy. A similar effect has been observed in the chlorination of methyl hydroperoxides, ROOH, studied by Sun et al.,[42] who showed that the successive chlorination of the methyl group resulted in an increasing stabilization of the corresponding hydroperoxides relative to the methyl hydroperoxide, CH$_3$OOH. In the same way, the iodination of the methoxy group increases the relative stability of the hydroperoxide derivative compared to methoxy iodoperoxide, CH$_3$OOOI.

Reaction Pathways. As shown in the energy profile (Figure 3), several chemical pathways are possible in principle, from the reaction CH$_3$O$_2$ + IO through the decomposition of the intermediate nascent association minima, CH$_3$OOOI and CH$_3$-OOIO. Since the experimental identification of the products has not been feasible, all plausible channels are investigated in order to have a most complete picture as possible of the mechanism of the reaction. Thus, in addition to the methyl iodate formation channel

$$CH_3O_2 + IO \rightarrow CH_3OOIO \rightarrow TS2 \rightarrow CH_3OIO_2$$

the following chemical pathways are suggested:

$$CH_3O_2 + IO \rightarrow CH_3OOOI \rightarrow CH_3O + IOO \qquad (a)$$

$$\rightarrow CH_3OOIO \rightarrow CH_3O + OIO \qquad (b)$$

$$\rightarrow CH_3OOOI \rightarrow TS4 \rightarrow CH_2O + HOOI \qquad (c)$$

$$\rightarrow CH_3OOIO \rightarrow TS5 \rightarrow CH_2O + HOIO \qquad (d)$$

$$\rightarrow CH_3OOOI \rightarrow TS6 \rightarrow CH_3OI + (^1\Delta)O_2 \qquad (e)$$

$$\rightarrow CH_3OOIO \rightarrow TS7 \rightarrow CH_3OI + (^1\Delta)O_2 \qquad (f)$$

$$\rightarrow CH_3OOOI \rightarrow TS8 \rightarrow CH_3I + O_3 \qquad (g)$$

$$\rightarrow TS9 \rightarrow CH_3OI + (^3\Sigma)O_2 \qquad (h)$$

The products CH$_3$O + IOO, CH$_3$O + OIO in channels a and b may be formed directly from the dissociation of the intermediate bound complexes, CH$_3$OOOI and CH$_3$OOIO, and are located below reactants at −4.3 (−3.2) and −8.2 (−7.7) kcal mol^{-1}, respectively, including the IO spin−orbit correction. CH$_3$O has been detected among the reaction products and IOO would be expected to decompose readily to I + O$_2$. Thus, channel a may be considered to be a possible reaction path as the corresponding CH$_3$O$_2$ + ClO → CH$_3$O + ClOO channel.[12,19] Iodine dioxide, OIO, has not been detected among the reaction products, suggesting a small branching ratio for channel b. Enami et al.,[9] concluded that the branching ratio for OIO formation is less than 0.1.

Before proceeding to the detailed examination of the remaining channels described in the above scheme, a close inspection of the energy profile (Figure 3) leads to an interesting observation. Regardless of the deviations observed among the relative energy results between the various methodologies, as listed in Table 3, the critical energy values for the various reaction channels fall into two major categories depending on the barrier

height that must be overcome. Indeed, there is a large energy gap between pathways that proceed through a low-energy barrier like TS4 and TS5 and the reaction channels that proceed through TS6, TS7, and TS8 and have to overcome the high critical energies associated. Transition states TS4 and TS5 are involved in channels c and d which lead to CH$_2$O + HOOI and CH$_2$O + HOIO through the decomposition of CH$_3$OOOI and CH$_3$OOIO, respectively. TS4 is formed due to the migration of a methylic hydrogen atom to the central oxygen atom at 1.436 (1.413) Å, the tightening of the C−O bond to 1.248 (1.255) Å and the breaking of the CO−O bond. The O−OI bond length decreases from 1.450 (1.428) Å in CH$_3$OOOI to 1.258 (1.276) Å in TS4 and the I−O bond increases from 2.035 (2.008) to 2.093 (2.088) Å in TS4. A widening of the IOO angle from 109.1° (110.5°) in CH$_3$OOOI to 118.9° (116.4°) in TS4 also takes place. The associated critical barrier is low located at 5.0 (5.6) kcal mol^{-1} above reactants, including the IO spin−orbit correction, which shows a non-negligible probability for this pathway. These products may further decompose to CH$_2$O + HI + O$_2$. A similar pathway has been established by Guha and Francisco[18] in the mechanism of the reaction CH$_3$O$_2$ + BrO. There too, a transition state analogous to TS4 has also been located after formation of the CH$_3$OOOBr association minimum, which leads to CH$_2$O + HOOBr products eventually decomposing to CH$_2$O + HBr + O$_2$. Even more probable appears to be the production of CH$_2$O + HOIO from CH$_3$OOIO through TS5. Similar to TS4, transition state TS5 involves the migration of a methylic H, the tightening of the C−O bond to 1.296 (1.295) Å, and the breaking of the peroxide bond. The critical energy to be overcome is also low located at 3.7 (4.1) kcal mol^{-1}, including the spin−orbit correction, above reactants. The low-energy barriers associated with TS4 and TS5 are consistent with the weak positive temperature dependence observed experimentally.[9] The CH$_2$O detection among the reaction products and the low critical energies calculated provide good evidence that these channels may dominate the mechanism of the reaction. Consequently, the decomposition processes c and d that lead to CH$_2$O + HOOI and CH$_2$O + HOIO products, eventually decomposing into CH$_2$O + HI + O$_2$, are suggested to be along with channel a, the significant reaction pathways.

The transition state configurations TS6 and TS7 lead to the stable products CH$_3$OI + ^{1}O$_2$ from the decomposition of CH$_3$-OOOI and CH$_3$OOIO, respectively. They involve the elimination of molecular oxygen and they are the only routes determined that yield methyl hypoiodide on the singlet surface. In TS6 the C−O and IO−O distances increase considerably to 1.891 (1.888) and 2.116 (2.018) Å, respectively. On the other hand the CO−O bond distance decreases to 1.365 (1.330) Å and the iodine connected oxygen atom approaches the carbon atom at 1.997 (1.987) Å. Similar geometrical changes take place in TS7 where the terminal oxygen approaches the carbon atom at 1.938 (1.926) Å and the C−OO and OI−O distances are elongated to 1.934 (1.952) and 2.443 (2.431) Å, respectively. Both transition states are very high located compared to the reactants and they are thus, quite analogous to the transition states for the reactions CH$_3$OOOBr → CH$_3$OBr + O$_2$ and CH$_3$OOBrO → CH$_3$OBr + O$_2$.[18] The energy order is similar too, with TS6 corresponding to the reaction CH$_3$OOOI → CH$_3$OI + O$_2$, located higher than TS7 corresponding to CH$_3$OOIO → CH$_3$OI + O$_2$, exactly as the energy order of the transition states for the reactions CH$_3$-OOOBr → CH$_3$OBr + O$_2$ and CH$_3$OOBrO → CH$_3$OBr + O$_2$. Experimentally,[8] CH$_3$OI has been suggested to be among the most likely products, in analogy with the CH$_3$O$_2$ + ClO system, where a substantial branching ratio for the CH$_3$OCl + O$_2$

(CH₃IO₃) Isomers and the CH₃O₂ + IO Reaction Pathways

J. Phys. Chem. A, Vol. 111, No. 17, 2007 **3407**

formation channel was measured.[13] However, the production of methyl hypochlorite, CH_3OCl, in CH_3O_2 + ClO has been suggested to occur via either the triplet state or the decomposition of CH_3OClO_2 minimum, assumed to be formed as an intermediate complex during the reaction.[19] In the present system no CH_3OIO_2 decomposition pathway has been determined and the particular stability of methyl iodate makes its dissociation to CH_3OI + O_2 very unlikely. Hence, the formation of methyl hypoiodide in the CH_3O_2 + IO reaction on the singlet surface appears questionable. A direct path leading to CH_3OI on the triplet state has been determined as we shall see below, but it also involves a high barrier.

The final reaction channel investigated on the singlet surface leads to iodomethane formation and the release of ozone. The corresponding transition state determined is TS8, a five-centered nonplanar structure which characterizes the decomposition process $CH_3OOOI \rightarrow CH_3I + O_3$. The geometrical features include a considerable elongation of C−O and O−I bonds to 2.858 (2.861) and 2.808 (2.775) Å, respectively relative to 1.432 (1.426) and 2.035 (2.008) Å in CH_3OOOI. Like the other transition states of higher energies, TS8 corresponds to a reaction channel of minor importance since the associated barrier energy is very high more than 50 kcal mol⁻¹ above reactants.

The exploration of the reaction on the triplet state has revealed a direct channel leading through the elimination of triplet molecular oxygen to methyl hypoiodide, CH_3O_2 + IO → CH_3-OI + $^3O_2$. The corresponding transition state determined, TS9, occurs due to the conjunction of the oxygen atom of the IO radical with the carbon atom of CH_3O_2 with the synchronous elimination of molecular oxygen. The C−O bond in TS9, 1.665 (1.654) Å, is much longer than the length of the C−O bond in the CH_3O_2 radical, 1.437 Å, leading to the eventual rupture of the C−O bond and the elimination of molecular oxygen from CH_3O_2. The O−O bond is shorter in TS9 than in CH_3O_2, 1.340 (1.318) Å, tending to the O−O bond distance in free O_2 (1.228) Å, and similarly the I−O bond in TS9, 1.996 (1.992) is longer than that in free IO, 1.868 Å.[32] The energy of TS9 is very high compared to reactants and excludes any possibility for CH_3OI formation on the triplet surface. We may conclude that formation of CH_3OI appears unlikely either on singlet or triplet surface.

4. Summary

The isomers of the (CH_3IO_3) family and the most important stationary points on the potential energy surface of the reaction between methylperoxy radicals and iodine monoxide have been investigated using quantum mechanical electronic structure methods based on all-electron and effective-core-potential treatments. Five isomeric structures in the family have been determined following the energy stability order: CH_3OIO_2 < ICH_2OOOH < CH_3OOOI ∼ CH_3OOIO < CH_3IO_3. The methyl iodate isomer, CH_3OIO_2, may be formed from the isomerization of CH_3OOIO via a low-energy barrier. It is found to be particularly stable with an estimated heat of formation value equal to −17.7 ± 2.4 (−16.9 ± 2.4) kcal mol⁻¹. Thus, it is likely to act as a sink compound for I in the marine boundary layer.

The mechanism of the reaction CH_3O_2 + IO is suggested to involve the intermediate formation of either of the nascent association minima CH_3OOOI, CH_3OOIO which are comparable in stability and may decompose to CH_3O + IOO, CH_3O + OIO, CH_2O + HOOI, and CH_2 + HOIO species, via low-energy barriers. On the other hand, the channels that yield methyl hypoiodide, CH_3OI, must overcome high critical energies and are not likely neither on the singlet or the triplet surface.

Comparison with the analogous reactions between the methylperoxy radical and chlorine and bromine monoxide shows a similar overall picture, although the detailed examination of the possible chemical pathways indicates a closer resemblance to the system CH_3O_2 + BrO[18] rather than to CH_3O_2 + ClO.[19] A notable difference occurs in the relative stabilities of the CH_3-OOBrO, CH_3OOClO isomers which are much higher located than the species CH_3OOOBr and CH_3OOOCl, opposite to the comparable iodine isomers CH_3OOOI, CH_3OOIO. Consequently, the reaction CH_3O_2 + IO, as already emphasized, may proceed through either association minimum, in analogy with the reaction HO_2 + IO.[25]

The comparison of the theoretical findings with the experimental reports is interesting. The computational study predicts low activation energies for the important channels a−d, which are consistent with the large values of the rate constant measured[8,9] and the slight positive temperature dependence observed experimentally.[9] On the basis of these results, the significance of the reaction CH_3O_2 + IO in atmospheric chemistry[8] is established. The considerably smaller values of the rate constant that have been recently measured[10] are not consistent with the atmospheric role of this system and the low-energy barriers calculated in the present work. This discrepancy indicates the complexity of the reaction CH_3O_2 + IO that deserves further investigation.

References and Notes

(1) O', Dowd, C. D.; Jimenez, J. L.; Bahreini, R.; Flagan, R. C.; Seinfeld, J. H.; Kulmala, M.; Pirjola, L.; Hoffmann, T. *Nature (London, U.K.)* **2002**, *417*, 632.

(2) McFiggans, G. *Nature (London, U.K.)* **2005**, *433*, 7026.

(3) McFiggans, G.; Allan, B.; Coe, H.; Plane, J. M. C.; Carpenter, L. J.; O', Dowd, C. *J. Geophys. Res.* **2000**, *105*, 371.

(4) von Glasow, R.; Sander, R.; Bott, A.; Crutzen, P. J. *J. Geophys. Res.* **2002**, *107*, 4341.

(5) Carpenter, L. J. *Chem. Rev.* **2003**, *103*, 4953.

(6) Saiz-Lopez, A.; Plane, J. M. C. *Geophys. Res. Lett.* **2004**, *31*, L04112.

(7) Vogt, R.; Sander, R.; von Glasow, R.; Crutzen, P. J. *J. Atmos. Chem.* **1999**, *32*, 375.

(8) Bale, C. S. E.; Canosa-Mas, C. E. Shallcross, D. E.; Wayne, R. P. *Phys. Chem. Chem. Phys.* **2005**, *7*, 2164.

(9) Enami, S.; Yamanaka, T.; Hashimoto, S.; Kawasaki, M.; Nakano, Y.; Ishiwata, T. *J. Phys. Chem. A* **2006**, *110*, 9861.

(10) Dillon, T. J.; Tucceri, M.; Crowley, J. N. *Phys. Chem. Chem. Phys.* **2006**, *8*, 5185.

(11) Simon, F. G.; Burrows, J. P.; Schneider, W.; Moorgat, G. K.; Crutzen, P. J. *J. Phys. Chem.* **1989**, *93*, 7807.

(12) Crutzen, P. J.; Müller, R.; Brühl, C.; Peter, T. *Geophys. Res. Lett.* **1992**, *19*, 1113.

(13) Helleis, F.; Crowley, J. N.; Moorgat, G. K. *J. Phys. Chem.* **1993**, *97*, 11464.

(14) Helleis, F.; Crowley, J.; Moorgat, G. *Geophys. Res. Lett.* **1994**, *21*, 1795.

(15) Daële, V.; Poulet, G. *J. Chim. Phys.* **1996**, *93*, 1081.

(16) Aranda, A.; Le Bras, G.; La Verdet, G.; Poulet, G. *Geophys. Res. Lett.* **1997**, *24*, 2745.

(17) Guha, S.; Francisco, J. S. *J. Phys. Chem. A* **2000**, *104*, 3239.

(18) Guha, S.; Francisco, J. S. *J. Chem. Phys.* **2003**, *118*, 1779.

(19) Drougas, E.; Kosmas, A. M. *J. Phys. Chem. A* **2003**, *107*, 11386.

(20) Jenkinn, M. E.; Cox, R. A.; Hayman, J. D. *Chem. Phys. Lett.* **1991**, *177*, 272.

(21) Maguin, F.; Laverdet, G.; Le Bras, G.; Poulet, G. *J. Phys. Chem.* **1992**, *96*, 1775.

(22) Canosa-Mas, C. E.; Flugge, M. L.; Shah, D.; Vipond, A.; Wayne, R. P. *J. Atmos. Chem.* **1999**, *34*, 153.

(23) Cronkhite, J. M.; Stickel, R. E.; Nicovich, J. M.; Wine, P. H. *J. Phys. Chem. A* **1999**, *103*, 322.

(24) Knight, G. P.; Crowley, J. N. *Phys. Chem. Chem. Phys.* **2001**, *3*, 393.

(25) Drougas, E.; Kosmas, A. M. *J. Phys. Chem. A* **2005**, *109*, 3887.

(26) Møller, C.; Plesset, M. S. *Phys. Rev.* **1934**, *46*, 618.

(27) Frisch, M. J.; Trucks, G. W.; Schlegel, H. B.; Scuseria, G. E.; Robb, M. A.; Cheeseman, J. R.; Zakrzewski, V. G.; Montgomery, Jr. J. A.; Stratmann, R. E.; Burant, J. C.; Dapprich, S.; Millam, J. M.; Daniels, A. D.; Kudin, K. N.; Strain, M. C.; Farkas, O.; Tomasi, J.; Barone, V.; Cossi, M.; Cammi, R.; Mennucci, B.; Pomelli, C.; Adamo, C.; Clifford, S.; Ochterski, J.; Petersson, G. A.; Ayala, P. Y.; Cui, Q.; Morokuma, K.; Malick, D. K.; Rabuck, A. D.; Raghavachari, K.; Foresman, J. B.; Cioslowski, J.; Ortiz, J. V.; Stefanov, B. B.; Liu, G.; Liashenko, A.; Piskorz, P.; Komaromi, I.; Gomperts, R.; Martin, R. L.; Fox, D. J.; Keith, T.; Al-Laham, M. A.; Peng, C. Y.; Nanayakkara, A.; Gonzalez, C.; Challacombe, M.; Gill, P. M. W.; Johnson, B.; Chen, W.; Wong, M. W.; Andres, J. L.; Head-Gordon, M.; Replogle, E. S.; Pople, J. A. *GAUSSIAN 98*, Revision A.9; Gaussian Inc.: Pittsburgh, PA, 1998.

(28) Sadlej, A. J. *Theor. Chim. Acta* **1992**, *81*, 339.

(29) Wadt, W. R.; Hay, P. J. *J. Chem. Phys.* **1985**, *82*, 284.

(30) Glukhovtsev, M. N.; Prossa, A.; Radom, L. *J. Am. Chem. Soc.* **1995**, *117*, 2024.

(31) Gonzalez, C.; Schlegel, H. B. *J. Chem. Phys.* **1989**, *90*, 2154.

(32) Gilles, M. K.; Polak, M. L.; Lineberger, W. C. *J. Chem. Phys.* **1991**, *95*, (4723).

(33) Buttar, D.; Hirst, D. M. *J. Chem. Soc., Faraday Trans.* **1994**, *90*, 1811.

(34) Knyazef, V. D.; Slagle, I. R. *J. Phys. Chem. A* **1998**, *102*, 1770.

(35) Bedjanian, Y.; Le Bras, G.; Poulet, G. *J. Phys. Chem. A* **1997**, *101*, 4088.

(36) Misra, A.; Berry, R. J.; Marshall, P. *J. Phys. Chem. A* **1997**, *101*, 7420.

(37) Plane, J. M. C.; Joseph, D. M.; Allan, B. J.; Ashworth, S. H.; Francisco, J. S. *J. Phys. Chem. A* **2006**, *110*, 93.

(38) Cotton, A. F.; Wilkinson, G. *Advanced Inorganic Chemistry*, 2nd ed.; Intersciences Publishers: 1967.

(39) Lee, T. J.; Dateo, C. E.; Rice, J. E. *Mol. Phys.* **1999**, *96*, 633.

(40) Papayannis, D. K.; Melissas, V. S.; Kosmas A. M. *Phys. Chem. Chem. Phys.* **2003**, *5*, 2976.

(41) Drougas, E.; Kosmas, A. M. *Int. J. Quantum Chem.* **2004**, *98*, 335.

(42) Sun, H.; Chen, C.-J.; Bozzelli, J. W. *J. Phys. Chem. A* **2000**, *104*, 8270.